

NUMERICAL ESTIMATION OF THE SPENT FUEL RATIO

Samuel G. Durbin, Eric R. Lindgren, Jason Wilke, and Kevin J. Jameson

Sandia National Laboratories, P.O. Box 5800, Albuquerque, NM 87123-1369 USA, sdurbin@sandia.gov

Sabotage of spent nuclear fuel casks remains a concern nearly forty years after attacks against shipment casks were first analyzed and has a renewed relevance in the post-9/11 environment. A limited number of full-scale tests and supporting efforts using surrogate materials, typically depleted uranium dioxide (DUO₂), have been conducted in the interim to more definitively determine the source term from these postulated events. In all the previous studies, the postulated attack of greatest interest was by a conical shape charge (CSC) that focuses the explosive energy much more efficiently than bulk explosives. However, the validity of these large-scale results remain in question due to the lack of a defensible Spent Fuel Ratio (SFR), defined as the amount of respirable aerosol generated by an attack on a mass of spent fuel compared to that of an otherwise identical surrogate. Previous attempts to define the SFR in the 1980's have resulted in estimates ranging from 0.42 to 12 and include suboptimal experimental techniques and data comparisons. Because of the large uncertainty surrounding the SFR, estimates of releases from security-related events may be unnecessarily conservative. Credible arguments exist that the SFR does not exceed a value of unity. A defensible determination of the SFR in this lower range would greatly reduce the calculated risk associated with the transport and storage of spent nuclear fuel in dry cask systems.

In the present work, the CTH shock physics code is used to simulate spent nuclear fuel (SNF) and DUO₂ targets impacted by a CSC jet at an ambient temperature condition. These preliminary results are used to illustrate an approach to estimate the respirable release fraction for each type of material and ultimately, an estimate of the SFR.

I. INTRODUCTION

A number of studies have been commissioned over four decades to estimate the source term and subsequent results of exposure from postulated attacks. In the late 1970's, a conservative analysis was published by Sandia National Laboratories (SNL).¹ Due to lack of experimental data, the study by DuCharme used expert judgment to define the amount of material released by an

attack in downtown Manhattan. As a result the US Nuclear Regulatory Commission (NRC) imposed new regulations requiring increased security for shipments of spent fuel to protect against sabotage events.

In response to the perceived conservatism in the report by DuCharme, a second analysis was conducted in an attempt to refine the assumptions made in the original assessment.² The estimated releases from this new study were 14 times lower than reported in the DuCharme report, but the NRC did not relax the interim regulations on the transportation of spent fuel at that time.

I.A. Previous Attempts to Measure the SFR

Acknowledging the lack of experimental data in this technical area, the NRC and DOE both funded parallel test programs to determine the source term from full-scale and scaled casks. The costs and safety requirements to conduct the full-scale tests with actual spent fuel would have been prohibitive. Therefore, the test planners at SNL chose to conduct the full-scale tests with fuel rods filled with surrogate pellets made of depleted uranium dioxide (DUO₂).³ DUO₂ was chosen in an attempt to best match the mechanical response of spent fuel interacting with a high energy device (HED) such as a conical shape charge (CSC). This substitution appears justified because spent fuel contains approximately 90% by mass of U-238 dioxide. However, actual spent fuel pellets contain several properties unique to irradiated fuel such as fission products, a fragmented structure, and embrittled cladding. The ability to scale the results of the full-scale sabotage tests for expected releases from actual spent fuel required the measurement of a spent fuel ratio (SFR). The SFR is defined as the ratio between the spent fuel respirable aerosol mass released to the DUO₂ surrogate respirable aerosol mass released under other otherwise identical, disruptive conditions. Respirable aerosols are defined as particles with an aerodynamic equivalent diameter (AED) less than 10 μm, which for UO₂ particles translates to a geometric diameter of 3.2 μm.

Subsequent large scale tests conducted by SNL and Gesellschaft für Anlagen- und Reaktorsicherheit (GRS, German Reactor Safety Authority) also elected to use DUO₂ as a fuel surrogate, further increasing the

importance of the SFR for accurate source term interpretation.^{4,5}

Two parallel programs, one at Battelle Columbus Laboratories (BCL) and another at Idaho National Engineering Laboratory (INL), were conducted in the early 1980's to obtain the SFR but resulted in inconclusive results.^{6,7} A follow-on effort was conducted in the 2000's at SNL, but funding was discontinued prior to testing with spent fuel.⁸

I.B. Microstructural Changes in Irradiated Fuel

The ceramic density is a key material property needed to describe fresh and SNF. The ceramic density throughout fresh fuel is initially uniform at between 95 to 96% of the theoretical maximum density of UO_2 (10.97 g/cm^3). During irradiation a number of physical phenomena change the fuel microstructure. Each fission event in the fuel produces two fission products. Some fission products are solids and others are gases. Both solid and gaseous fission products contribute to fuel swelling that reduces the fuel ceramic density. After an initial period of slight densification at low burnup (< 15 GWd/MTHM), the density of the fuel pellet decreases linearly with burnup.⁹

The grain size in fresh fuel is typically in the range of 10 to 20 μm .¹⁰ As the fuel is irradiated to high burnup (> 60 GWd/MTHM), the grain size decreases significantly (~0.3 μm) concomitant with the formation of small (~0.5 μm) pores.^{11,12} Calculated pore pressures in these small pores in high burnup fuel range from 100 to 500 MPa and are considered to be partly responsible for the pellet swelling.¹²

As stated previously, the UO_2 particles of interest have geometric diameters less than 3.2 μm . Ductile materials characteristically fracture along the grain boundaries (intergranular fracture). If high burnup SNF and surrogate materials were to behave as ductile materials, the small grain size of irradiated fuel would result in a greater release of respirable aerosols than the larger grained fresh fuel. This behavior would lead to a SFR significantly greater than unity. However, UO_2 behaves as a brittle material at temperatures below 1900 K, the brittle-ductile transition temperature.¹³ Below 1900 K, fracture of the fuel pellets occurs through the grains (intragranular fracture) resulting in respirable aerosol release that is independent of grain size. An inherent assumption in the CTH modeling approach for this work is that the fracture characteristics of surrogate and irradiated fuel are similar and not dependent on grain size. The validity of this assumption is reviewed in the results section to verify that the fracture temperature is below the brittle-ductile transition temperature of 1900 K.

II. MODELING OF THE SPENT FUEL RATIO

The CTH hydrocode was chosen to study the reaction of spent nuclear fuel (SNF) and DUO_2 under loadings imparted by an HED. CTH is an explicit Eulerian code developed by SNL for solving high strain transient dynamics problems including shaped charges, explosions, and high velocity impact problems. The code can be run in one, two, or three dimensions. CTH has a large internal library of equation of state (EOS) data, including SESAME and ANEOS tabular forms. These EOS libraries track heating, liquefaction, and vaporization of materials, as well as solid phase changes caused by high pressure. CTH allows the user to choose from a variety of constitutive models for strength and fracture or failure models. Also, developer models are available that allow the user to build custom constitutive models. The code will run on workstations or cluster computers using from one to over 100,000 processing cores in parallel. An adaptive mesh capability allows the user to select which components of a problem to finely resolve. CTH can read in a variety of geometry file formats and generates output data files that may be studied using several different post-processing and visualization codes.

II.A. CTH Model Description

The CTH modeling domain simulating an ambient temperature experiment is shown in Figure 1. For these preliminary calculations the CSC jet is represented by a copper cylinder 20 mm long by 2 mm diameter with a velocity of 7.8 km/s and is depicted to the left of the target. The target is centered in the domain and is composed of a stack of five UO_2 pellets each 15.2 mm tall and 9.3 mm diameter inside of a 10.7 mm OD Zircaloy tube with 0.62 mm wall thickness. The initial density of the surrogate DUO_2 was set to 9.87 g/cc for these preliminary calculations, which is recognized to be lower than prototypic. The copper jet strikes the middle of the center pellet in the model. Figure 2 shows energy density as the jet strikes the target at 2, 4, 8, and 16 μs . Nearly all of the energy of the rod is deposited in the center pellet.

The material properties of spent fuel are studied by parametrically modifying the DUO_2 properties. The effect of density was explored in these preliminary calculations by reducing the initial density to 9.7 and 9.5 g/cc . The effect of increased brittleness, which is characteristic of SNF, was investigated by changing the failure strain in the constitutive model from 8% to 4%.

In a separate treatment, the surrogate and spent fuel pellets were treated as a porous material with effective densities of 9.7 and 9.5 g/cc . This porous material must first undergo compaction of the pore space before undergoing compression of the solid component along the Hugoniot curve, which describes the material pressure as a function of specific volume. The Rankine-Hugoniot

jump equations relationships are used to relate pressure and density to particle velocity and shock velocity. The compaction of the porous material was treated using the P-alpha model. For the P-alpha model, the user specifies a porous density, initial porous crush pressure, and a final crush pressure required to compact the foam to a solid material. After this point, the material is again modeled as a solid using the Mie-Grunieson EOS. For these preliminary simulations, the initial crush pressure and final crush pressure were assumed to be 1034 and 3447 MPa, respectively.

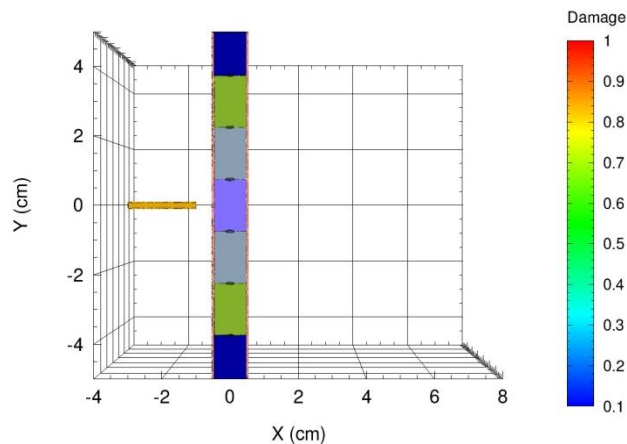


Fig. 1. Modeling domain in CTH.

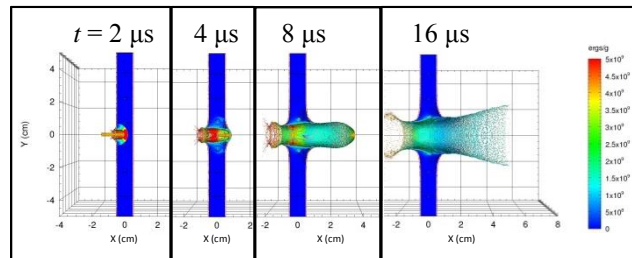


Fig. 2. Energy density at $t = 2, 4, 8,$ and $16 \mu\text{s}$.

II.B. Estimation of Respirable Fraction

The numerical simulations do not need to directly determine the particle size distribution produced by the interaction. Previous studies have postulated that the respirable release fraction is a function of energy density such as shown in Figure 3, where the respirable release fraction is assumed to be particles equal to or smaller than $10 \mu\text{m}$ aerodynamic equivalent diameter (AED).¹⁴ The data represented in Figure 3 are taken from various sources and include glasses, vitrified waste forms, DUO_2 , and limited samples of SNF.^{7,8,15,16} The burnup of the SNF samples is shown in gigawatt-days per metric ton of heavy metal (GWd/MTHM).

For these studies the data of most interest are those for DUO_2 and SNF. These data are replotted and fitted in Figure 4. From this relationship the respirable release

fraction generated by a disrupted pellet can be calculated from the energy density imparted to the pellet.

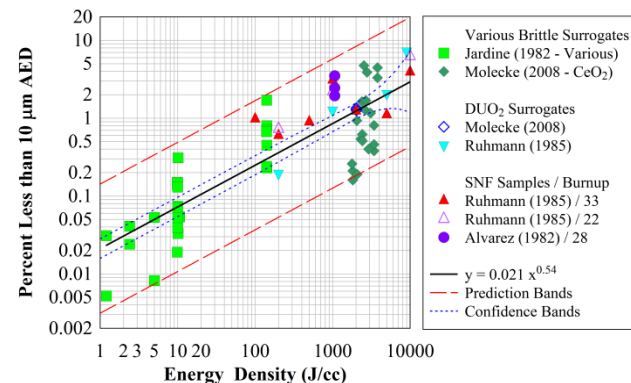


Fig. 3. Mass of aerosols with aerodynamic equivalent diameter (AED) $< 10 \mu\text{m}$ normalized by affected mass as a function of energy density.

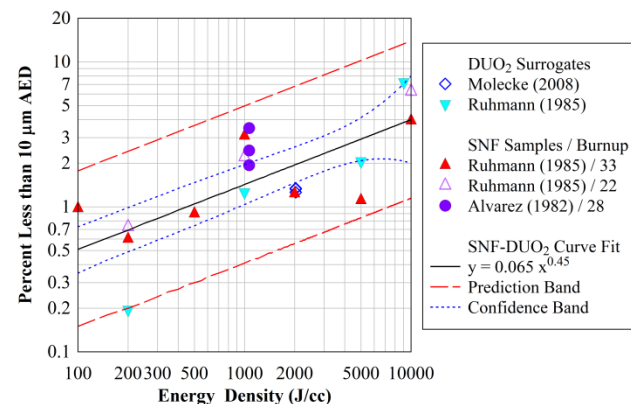


Fig. 4. Mass of SNF and DUO_2 aerosols with aerodynamic equivalent diameter (AED) $< 10 \mu\text{m}$ normalized by affected mass as a function of energy density.

III. PRELIMINARY RESULTS

The increase in internal energy density of the middle pellet was used to estimate the respirable release fraction. Figure 5 shows the internal energy increase with time for the base case (DUO_2) and several simulated SNF materials. The initial sharp peak in internal energy is due to high pressures associated with the passage of the shock wave through the pellet. After the shock wave leaves the pellet, the internal energy density for the DUO_2 case increases to a plateau value which peaks to 925 J/cc at about $27 \mu\text{s}$. This plateau energy is imparted into the pellet because the material follows the Rayleigh jump line at the shock front and then the pressure-volume Hugoniot line during subsequent pressure decay. The Rayleigh line and Hugoniot enclose an area in the pressure-volume Hugoniot plane, which corresponds to the imparted

energy. Using this energy density in the correlation in Figure 4 predicts a respirable release percentage of 1.4%.

For the density sensitivity cases, the pellet initial density was decreased to 9.7 and 9.5 g/cc in the Mie-Gruneisen EOS. The internal energy density reached values of 924 and 910 J/cc for the 9.7 and 9.5 g/cc cases, respectively. The failure strain was reduced by a factor of two for the brittle sensitivity case. This reduction in ductility resulted in a plateau internal energy density of 923 J/cc. The changes in initial density and fuel ductility explored in this preliminary study did not have a significant effect on the energy imparted to the target material.

The largest increase in energy density was realized by reducing the pellet density using the P-alpha model. The internal energy densities were 1030 and 1180 J/cc for the 9.7 and 9.5 g/cc cases, respectively. Treating the ceramic as a crushable, porous material increases the internal energy of the target material while reducing its kinetic energy. This is because work is performed on the material as the pore space is compacted. However, these results for crushable SNF are preliminary as the parameters currently used in the P-alpha model have not yet been validated for spent fuel.

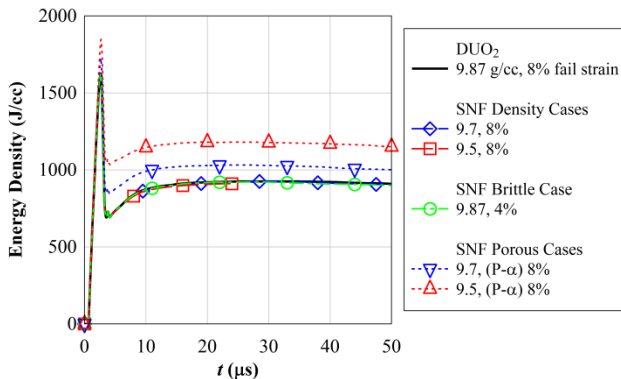


Fig. 5. Internal energy density of the central pellet for different modeling cases.

The average temperature of the pellet during fracture can be estimated from the energy density, thermal mass, and initial temperature of the pellet. The initial temperature for the simulations shown here is 298 K, which models an ambient temperature experiment. The average $\rho \cdot C_p$ of UO_2 between 298 K and 700 K is 2.8 J/(cc·K), which would result in a temperature increase of about 414 K for the highest calculated energy density of 1180 J/cc.¹⁷ Therefore, the estimated temperature during fracture is 712 K, which is well below the 1900 K brittle-ductile transition temperature.¹³ Again, fractures below this transition temperature are dominated by intragranular breakup and provide a plausible mechanism by which SNF and DUO_2 surrogates may be characterized by similar respirable releases.

This argument also extends to SNF should this type of fracture occur under storage conditions. In this situation, a conservative upper limit of the temperature of a fuel pellet in dry storage is 673 K. The average fracture temperature for SNF would then be 1053 K, which is still well below the transition temperature.

Table I summarizes the results for all modeling cases in this study. As discussed previously, the largest changes to energy density were observed for the cases using the porous P-alpha model. The SFR was calculated by dividing the respirable percentage for the SNF cases by the respirable percentage from the DUO_2 case. The P-alpha cases both produced an SFR of 1.1. These results should be considered preliminary. A broader treatment of the parameter space is underway, and assumptions in the material characteristics still require validation. However, these early results indicate that arguments for an SFR approaching unity appear to be justified.

TABLE I. Spent Fuel Ratio for All Modeling Cases.

	Density (g/cc)	Energy Density (J/cc)	Resp. (%)	SFR
DUO_2 (Base Case)				
	9.87	925	1.4	--
SNF: Density Cases				
	9.7	924	1.4	1.0
	9.5	910	1.4	1.0
SNF: Brittle Case				
	9.87	923	1.4	1.0
SNF: Porous Cases (P-alpha)				
	9.7	1030	1.5	1.1
	9.5	1180	1.5	1.1

IV. CONCLUSIONS

A modeling and simulation effort was commenced to explore the determination of a defensible SFR. These efforts combine the capabilities of the CTH shock-physics code with the available empirical data for respirable particle production of DUO_2 and SNF samples under high-energy loadings.

Preliminary results presented in this paper indicate that an SFR of unity appears to be justified. However, additional studies are ongoing that will investigate a wider set of mechanical properties for simulated SNF. In addition, treatments of material characteristics in the P-alpha model require validation. Other, porous models may also be evaluated in future work.

ACKNOWLEDGMENTS

This work was funded by the U.S. Department of Energy, Office of Nuclear Energy Fuel Cycle Technologies R&D Program through the Materials

Protection, Accounting, and Control Technologies (MPACT) campaign.

REFERENCES

1. A. R. DUCHARME, ET AL., "Transportation of Radionuclides in Urban Environs: Working Draft Assessment," Sandia National Laboratories, Report SAND77-1927, (1978).
2. N. C. FINLEY, ET AL., "Transportation of Radionuclides in Urban Environs: Draft Environmental Assessment," Nuclear Regulatory Commission, NUREG/CR-2472, (1980).
3. R. P. SANDOVAL, ET AL., "An Assessment of the Safety of Spent Fuel Transportation in Urban Environs", Sandia National Laboratories, Report SAND82-2365, (1983).
4. J. S. PHILBIN, ET AL., "Behavior of a Simulated, Metal Spent-Fuel Storage Cask under Explosive Attack," Sandia National Laboratories, Report SAND87-2358C, (1988).
5. F. LANGE, ET AL., "Experimental Determination for UO₂ Release from a Spent Fuel Transport Cask after Shaped Charge Attack," Proc. INMM 35th Meeting, Naples, Florida, July 17-20, (1994).
6. E. W. SCHMIDT, ET AL., "Final Report on Shipping Cask Sabotage Source Term Investigation," BMI-2095, NUREG/CR-2472, Battelle Columbus Laboratory, Columbus, OH, (1982).
7. J. L. ALVAREZ, ET AL., "Waste Forms Project: Correlation Testing", Idaho National Engineering Laboratory Report EGG-PR-5590, (1982).
8. M. A. MOLECKE, ET AL., "Spent Fuel Sabotage Test Program, Characterization of Aerosol Dispersal: Interim Final Report", Sandia National Laboratories, Report SAND2007-8070, (2008).
9. S. CARUSO, "Characterisation of High-Burnup LWR Fuel Rods through Gamma Tomography", PhD Thesis No. 3762, École Polytechnique Federale de Lausanne (EPFL), Switzerland, (2007).
10. J. NOIROT, ET AL., "High Burnup Changes in UO₂ Fuels Irradiated up to 83 GWD/T in M5[®] Claddings", *Nucl. Eng. Technol.*, **41** NO. 2, Special Issue on the Water Reactor Fuel Performance Meeting, (2009).
11. C. T. WALKER, ET AL., "Concerning the Microstructure Changes that Occur at the Surface of UO₂ Pellets on Irradiation to High Burnup", *J. Nucl. Mater.*, **188**, 73-79, (1992).
12. Y. H. KOO, B. H. LEE, J. S. CHEON, and D. S. SOHN, "Pore Pressure and Swelling in the Rim Region of LWR High Burnup UO₂ Fuel," *J. Nucl. Mater.*, **295**, 213-220, (2001).
13. A. W. CRONENBERG and T. R. YACKLE, "Intergranular Fracture of Unrestricted UO₂ Fuel during Film-Boiling Operation," *J. Nucl. Mater.*, **84**, 295-318 (1979).
14. S. G. DURBIN and R. E. LUNA, "A Methodology to Quantify the Release of Spent Nuclear Fuel from Dry Casks during Security-Related Scenarios," Sandia National Laboratories, SAND2013-9684, (2013).
15. L. J. JARDINE, ET AL., "Final Report of Experimental Laboratory Scale Brittle Fracture Studies of Glasses and Ceramics," Argonne National Laboratory, Report ANL-82-39, (1982).
16. H. RUHMANN, ET AL., "Research Program on the Behavior of Burnt-Up Fuel under Strong Mechanical Impacts," Kraftwerk Union, Report R 917/85/002, (1985).
17. S. G. POPOV, V. K. IVANOV, J. J. CARBAJO and G. L. YODER, "Thermophysical Properties of MOX and UO₂ Fuels Including the Effects of Irradiation," ORNL/TM-2000/351, (2000).